

Bridging carrier transport and amorphous dynamics in phase change materials

Andrea L. Lacaita[§] and Daniele Ielmini

Dipartimento di Elettronica e Informazione and IU.NET, Politecnico di Milano, Milano, Italy

phone +39 02 2399 6117, fax +39 02 236 7604, e-mail andrea.lacaita@polimi.it

^(§) also with IFN-CNR, Milano, Italy

(invited paper)

ABSTRACT

Physics of amorphous chalcogenides sets the scaling potentials of PCM elements and their perspectives in multi-bit storage. Carrier transport, threshold switching, structural relaxation and crystallization processes have key importance from the application standpoint. They also represent peculiar effects which have always attracted interest and speculations by decades. The paper reviews experimental and modeling analysis of threshold voltage and resistance transients in amorphous chalcogenides. Both variables show time evolutions characterized by a fast component in the 10's of ns range, called recovery, followed by a slower drift on longer time scales, with a gradual increase of the amorphous resistivity and activation energy. This latter dependence, ascribed to structural relaxations (SR) in the amorphous, proceeds until crystallization takes place. Although these processes appear rather different, the Poole Frenkel model of carrier conduction in disordered materials is remarkably able to link consistently them all, explaining the kinetics over 17 decades of time. Moreover, the Arrhenius dependence of SR shows that the exponential pre-factor of the process obeys a Meyer–Neldel rule, pointing to many-body thermal excitations as responsible for the anomalous large values of the crystallization time pre-factor observed in chalcogenide glasses.

Key words: Chalcogenide materials, nonvolatile memories, phase-change memories (PCMs), threshold switching, Structural relaxation, Crystallization, Meyer–Neldel rule

1. INTRODUCTION

While charge storage memory concepts are facing fundamental scaling limits, industry is gaining confidence in the adoption of Tellurium-based programmable resistors as basic components for high-density solid-state storage media [1, 2]. Phase change memories (PCMs) have already reached the commercial stage and are playing as both a sustaining and a disruptive technology [3]. On the sustaining side, PCMs are contributing to performance and reliability improvement of low-power memory subsystems, providing flexibility and new design opportunities as high-performance read-mostly memory block. On the other hand, PCMs promise to be the revolutionary replacement of mainstream charge storage technologies as the downsizing trend will approach the 10 nm nodes [4, 5].

PCMs performance and reliability strictly depend on physics of disordered materials. Device engineering and product qualification need detailed understanding and quantitative knowledge of key peculiar effects such as carrier transport, threshold switching, structural relaxation (SR) and crystallization dynamics. However, despite the wealth of literature devoted to their investigations since the 60's, only recently a coherent framework explaining most of the material and device performance is beginning to emerge. A relevant contribution to these advances has been given by the reliable fabrications of multi-million nanoscale samples made possible by the industrial interest in this technology.

In this frame, the paper reviews the scientific path followed by our research group in the last years. Starting from the careful characterization of industrial-grade $\text{Ge}_2\text{Sb}_2\text{Te}_5$ (GST) PCMs a physically-based quantitative framework has been developed. The model provides a coherent explanation of a large set of data and offers a conceptual link between all the relevant PCM phenomena (amorphous conduction, threshold switching, structural relaxation and crystallization). Its ability to predict conduction, programming and reliability performance makes the model a powerful tool for PCM design and qualification and a basis for further refinements.

2. THRESHOLD SWITCHING, AMORPHOUS MICROSCOPIC STRUCTURE AND RECOVERY

Since its first discovery in the 60's [6], the explanation of threshold switching in chalcogenides has attracted a lot of interest and many models have been proposed in past and more recent literature [7-12]. The effect is characterized by a sudden *snapback* in the I-V of the amorphous cell (Fig. 1) and occurs when a *threshold switching voltage* is exceeded. From the application standpoint *threshold switching* is a key effect, since it makes possible to abruptly *switching* the amorphous chalcogenide to a high conductive state, thus reaching with a bias on a few Volts, the currents needed for melting. Threshold voltage sets also the critical boundary to safely read the cell state without perturbing it, while the switching dynamics determines the ultimate device programming speed and the switching statistics contributes to the resistance spread resulting from program operation. [13]

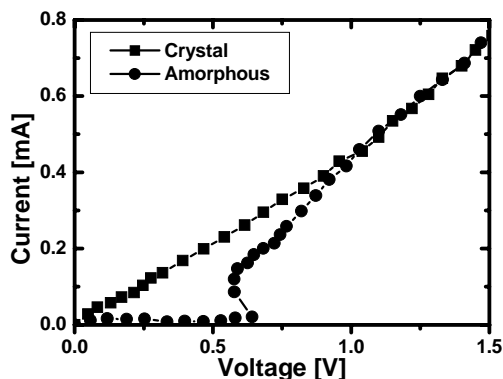


Fig. 1 – I-V curve of a GST PCM cell in the crystalline and in the amorphous states.

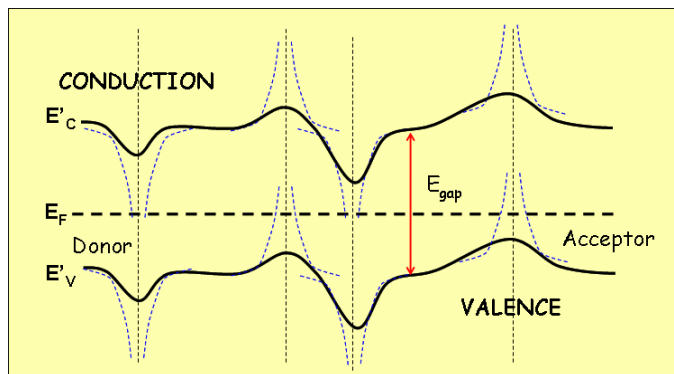


Fig. 2 – Schematic representation of conduction and valence band edges in the amorphous with potential fluctuations, effective donor/acceptors-like states

Since the late '70s relevant scientific literature [7, 8] has been ascribing threshold switching to a pure electronic process due to a positive feedback in carrier transport which makes conductivity of disordered materials eventually switching to a high value. In this frame, two conditions are essential for the switching to take place: (i) the presence of a large trap density and (ii) carrier conductivity exponentially dependent on field. Amorphous materials definitely meet the first requirement. Their disordered atomic structure leads to a large concentration of localized states for both electrons and holes with a random distribution in space and in energy (Fig. 2). [14-18] It has become thus a common practice to describe these materials as characterized by *mobility edges* which are separating fully de-localized bands from low mobility states. [14,19] Depending on their potential profiles, these localized levels may be divided into two categories, the trap-like levels (i.e. neutral when empty) and donor /acceptor-like levels (neutral when occupied by an electron/hole). A trap density in the gap of some 10^{20} - 10^{21} cm^{-3} , and a much lower, but still significant, donor/acceptor density, 10^{18} - 10^{19} cm^{-3} are usually suggested by the experiments [18]. In the following we will refer to donor/acceptor states as Coulomb states with density, N_T . Their large density pins the Fermi level in the middle of the energy gap, leading to the high amorphous resistivity and to the large activation energy for conduction. Values in the range 0.22-0,38eV are typical of GST devices [19].

Figure 3 shows the I-V curve of an amorphous PCM GST cell in a logarithmic scale, to emphasize the conduction features before switching. The ohmic dependence at low bias is followed by an exponential rise of the current which can be explained by thermally-activated hopping and Poole-Frenkel (PF) carrier emission from Coulomb states [17]. It is well known that the barrier lowering of a Coulomb potential decreases as the square root of the electric field. A PF effect is therefore expected to account for a current exponentially dependent on the square root of voltage. However, if the density of Coulomb sites approaches the values above, they interfere with each other. The peak of the potential barrier occurs close to the mid distance of the closest neighbors and its height decreases proportionally to the field intensity. In this limit the current through an amorphous region of thickness u_a is given by: [11]

$$I = 2qAN_T \frac{\Delta z}{\tau_0} e^{-\frac{E_C - E_F}{kT}} \sinh\left(\frac{qV}{kT} \frac{\Delta z}{2u_a}\right) \quad (1)$$

where q is the elementary charge, A the device cross section, τ_0 is the attempt to escape time for a trapped carrier, N_T is the density of Coulomb states between the Fermi level E_F and the conduction-band mobility edge E_C , while Δz is the average distance between them. Equation (1) has two relevant limits which are derived by expanding the sinh function at small and large voltages.

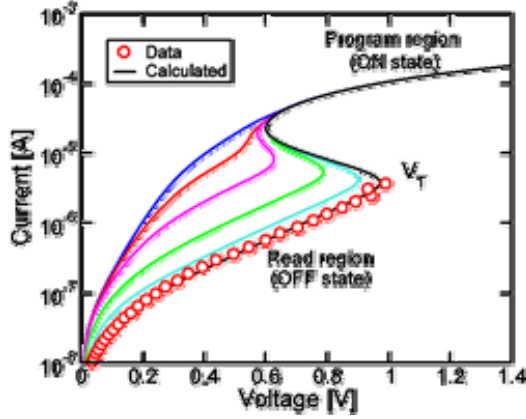


Fig. 3 - Calculated curve for a PCM device in the reset state. The read (subthreshold) and programming (ON) regimes are shown.

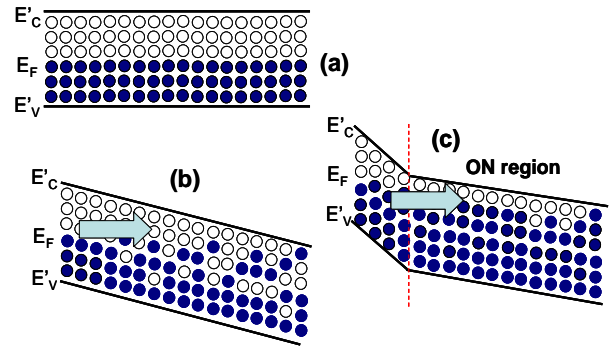


Fig. 4 – Schematic dependence of the band-edges and of the Fermi level in the amorphous chalcogenide resistor (a) at equilibrium; (b) before switching, (c) after switching.

In the low voltage regime, conduction is ohmic with a resistance featuring an activation energy given by $(E_C - E_F)$. At large voltage, the Poole-like dependence is readily recovered. [11]. The corresponding equations read as:

$$R = \frac{kT\tau_0 u_a}{q^2 AN_T \Delta z^2} e^{-\frac{E_C - E_F}{kT}}, \quad \log\left(\frac{I}{I_0}\right) \propto -\frac{E_C - E_F - qV\Delta z/2u_a}{kT} \quad (2)$$

Simple geometric considerations link Δz to N_T as $\Delta z = 0.55 (N_T)^{-1/3}$. Therefore donor/acceptor state densities in the 10^{17} - 10^{19} cm^{-3} range correspond to an average distance of $\Delta z = 5$ - 10 nm . Figure 3 shows the comparison between the experimental and the computed curve. The agreement is reached by taking $\Delta z = 5 \text{ nm}$. Equation (2b) also predicts that the activation energy for conduction should linearly decrease with voltage. The effect was indeed confirmed by experiments performed on GST PCM cells, thus contributing to build up confidence on the correctness of these initial model ingredients. [11, 20]

The same framework is able to account for threshold switching, reaching a remarkable quantitative agreement with the experiments. [11] Fig. 4 helps in describing how the high density of localized states and the exponential field dependence of PF conductivity interplay to cause the switching. While at low bias the amorphous acts as an ohmic resistor, at intermediate bias the overall current is set by the equilibrium between two regions. At the contact side, carriers are injected into intra-gap localized states by the electric field. Farther from the contact, the electric field heats-up the carriers into states closer to the band-edge, thus largely increasing the conductivity (Fig. 4b). Switching takes place when the exponential rise of the carrier conductivity in the amorphous bulk (ON region) makes possible to sustain the current injected through the contact barrier at a lower bias (Fig. 4c). In this regime, the carriers populating the states close to the band-edge in the ON region are provided by current injection from the contact side and charge storage is set by a steady-state balance with carrier recombination.

The model is able to account for the experimental dependence of the switching voltage on the thickness of the amorphous region and to for the almost constant value of the switching current in PCM cells. [21] Moreover, it makes possible to explain the transient recovery after switching without calling for any additional effect. As the voltage bias across the switched amorphous is switched off, it takes some time for the equilibrium state (Fig. 4a) to be restored. Carriers must leave the states close to the mobility edge while the Fermi level relaxes to the initial mid-gap position. The process time scale depends on the average escape/recombination time of carriers populating the traps.

Figure 3 shows the transient I-V curves computed by taking into account the finite Fermi level relaxation time in the amorphous. During the recovery, the I-V curve changes, the low field conductivity drops and the threshold switching voltage, V_T , increases. Figures 5 (a) and (b) show the excellent agreement achieved with the experimental results by taking a 5ns relaxation time. [13]

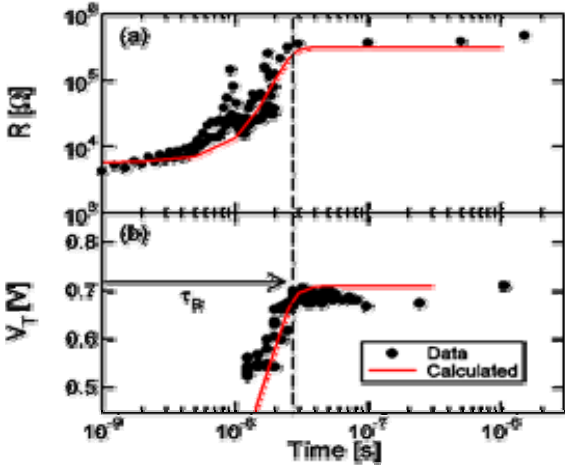


Fig. 5 - Measured and calculated dependence for (a) the low field resistance, R , and (b) threshold switching voltage, V_T , as a function of time after the end of a programming pulse. [13]

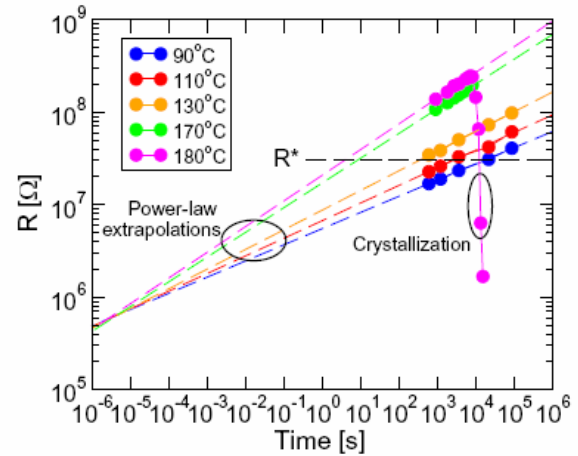


Fig. 6 – Experimental values of the low-field resistance R as a function of time for increasing annealing temperature, from 90 to 180 °C [48]

Before 10ns the I-V curve does not show a clear threshold switching voltage. It takes about 30ns for the high resistive state to be reached and for the snap-back shape to be recovered. In practice the correct cell resistance can be read only after about 50ns. This value adds to the overall PCM writing time.

3. STRUCTURAL RELAXATION AND CRYSTALLIZATION

Amorphous crystallization and structural relaxation (SR) mechanisms have a key impact on PCM cell reliability. Spontaneous crystallization is responsible of data loss. It is evident in Fig. 6 as the sudden resistance drop during the bake at 180°C. From the microscopic standpoint crystallization in GST implies first nucleation, which is a rearrangement of the atomic bonding in amorphous clusters, and then growth of the crystalline grain. Thus, the activation energy of about 2.6eV observed for GST crystallization is related to both the energy barrier for the formation of a critical nucleus and to the thermal activation of the growth process. [22, 23] On the other hand, before dropping due to spontaneous crystallization, the resistance of an amorphous layer shows a clear rise (Fig. 6) which follows a phenomenological power law given by [19, 24]:

$$R = R_0 \left(\frac{t}{t_0} \right)^\nu \quad (3)$$

Interestingly, all the extrapolations in Fig. 6 cross at $t_0=1\mu\text{s}$ and $R_0=400\text{ k}\Omega$. Considering the wide extrapolation time interval over 8 decades, both these values are not far from the recovery time and the initial resistance of the amorphous cell after recovery shown in Fig. 5.

The resistance drift can find a coherent explanation within the microscopic framework described above to explain amorphous conduction. Structural relaxation has been reported in a large variety of materials, from metallic glasses [25] to semiconductors like Si, [26] Ge [27], SiC [28] as well as in chalcogenides [29-32]. Differential scanning calorimetric experiments clearly show that SR is exothermic [26], while photoconductivity in amorphous Se indicates a power-law decrease of trap density [30]. These evidences suggest linking SR to defect annihilation events which causes a decrease of the localized state density, an increase of the mobility gap and via Eq. (2) an increase of the low field resistance.

Equation (2b) gives a straightforward way to test the picture against experimental results. Figure 7 compares the subthreshold I-V curve of a GST cell just after programming and after a bake at 120°C for 1day. The bake accelerates SR and, after bake, the low-field resistance is larger. More interestingly, the slope of the exponential current shape has clearly changed. The slope value, defined as STS=dV/dlog(I), can be derived from Eq.(2b) and found proportional to the average distance Δz between Coulomb centers [11]. The STS increase is therefore consistent with the Δz increase and with the idea that drift and its bake acceleration is accompanied by a decrease of the localized state densities. The variations of the low-field resistance can be accounted for by using Eq. (2a) and assuming that the shift of the mobility edge is described by:

$$\Delta(E_C - E_F) \approx -\chi \cdot \Delta N_T \quad (4)$$

Where $\chi=1.5 \times 10^{-19} \text{ eVcm}^3$ and the N_T variations can be experimentally derived from STS measurements of the I-V curves. Last but not least, according to the switching model in Fig. 4, the mobility edge controls V_T which, in fact, increases after drift (Fig. 7).

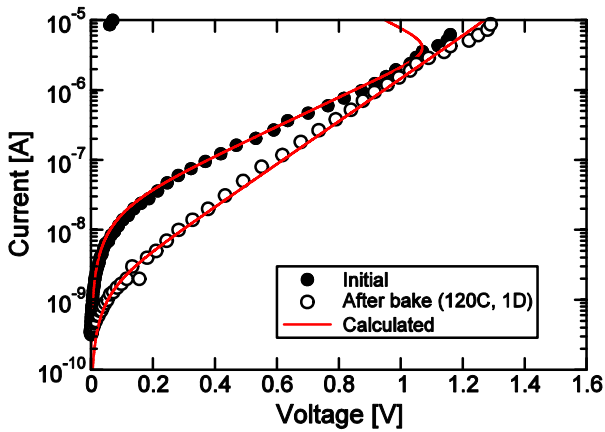


Fig. 7 – Experimental I-V curves measured at room temperature before and after an annealing for 1 day at T=120°C. Calculations were performed according to the PF conduction model [35]

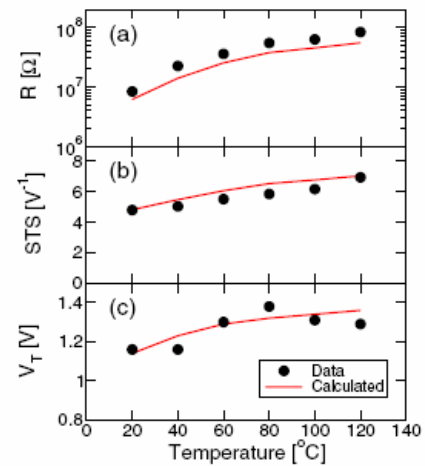


Fig. 8 – Experimental and calculated values for R (a), STS (b) and V_T (c) as a function of bake temperature [35].

Figure 8 shows the comparison between experimental and computed values of these quantities derived after bake on PCM cells at different temperatures [35]. The numerical estimates have been obtained using: (i) a description of the mobility edge shift equivalent to the one reported in Eq. (4); (ii) a kinetic model for defect annihilation. The latter is essential to estimate the N_C values at the end of the bake time at a given temperature. Since defects in the amorphous are metastable states, their relaxation to equilibrium has been described assuming a thermal excitation over an energy barrier, thus writing the average annihilation time τ of each defect as [31, 33]:

$$\tau = \tau_{at} e^{\frac{E_d}{kT}} \quad (5)$$

Where τ_{at} is the attempt to escape time set by atomic vibrations, and E_d is the activation energy. The disordered atomic structure of the amorphous suggests assuming the presence of a large variety of defects with E_d values broadly distributed over a large range. This assumption is consistent with the large range of time and temperature over which the power law drift can be observed, which entail a large variety of defects with relaxation times differing by many orders of magnitudes [34]. The computed curves in Fig.8 have been obtained taking for all defects $\tau_{at}=10^{-13}$ s in Eq.(5), a distribution of defect activation energies exponentially decreasing with E_d and a mobility edge dependence on N_C equivalent to the one given by Eq. (4) [24, 36]. The shape of the defect activation energy distribution is not critical. The experimental results can be also accounted for by using a distribution with a constant defect density up to the crystallization energy $E_x=2,6$ eV [22, 23]. This latter model distribution has a physical ground. In fact, crystallization may be seen as a limit of SR process. In both cases atomic rearrangements takes place, the only difference being that SR involves relaxation of some distorted, weak bonds while crystallization brings the whole defective cluster (the critical nucleus) to relax to an ordered structure. In both cases the process requires thermal excitation of bound carriers. Since SR involves thermal excitation of carriers that are localized in weak bonds, the activation energies of these processes are expected to be lower than E_x , which corresponds instead to carriers thermally excited from valence states.

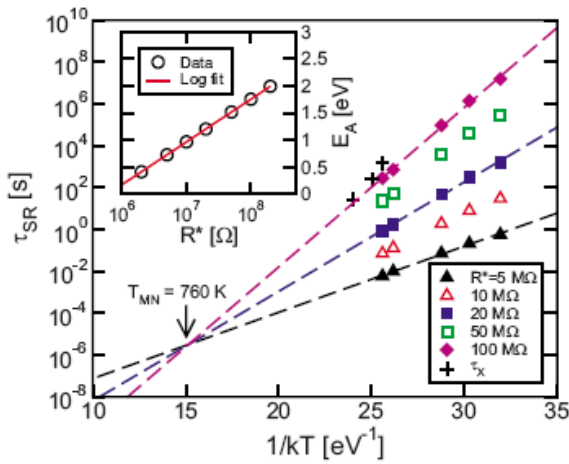


Fig. 9 - Arrhenius plot of the time-to-relaxation τ_{SR} , defined as the time to reach a given R value. Values of crystallization times t_x are also shown [46].

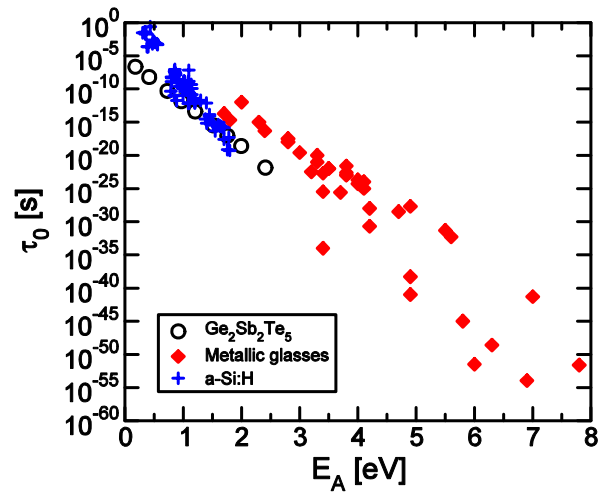


Fig. 10 - Correlation between Arrhenius pre-factor τ_0 and activation energy E_A following a Meyer–Neldel relationship. [46]

The continuous conceptual bridge existing between SR and crystallization is indeed confirmed by studying the activation energy of the data in Fig. 6. Taking a value R^* as a reference, an effective relaxation time τ_{SR} can be defined as the time to reach R^* . Figure 9 shows the extracted τ_{SR} in an Arrhenius plot, for R^* spanning from 5 to 100 M Ω . It turns out that τ_{SR} times follows an Arrhenius law like the one in Eq.(5) with an average activation energy linearly increasing with the logarithm of R^* , as demonstrated in the inset of Fig. 9. The continuous distribution of E_A is not surprising and is consistent with the disordered nature of the amorphous material. However the Arrhenius extrapolations in Fig. 9 say something more. All of them cross at the same point, namely at a temperature $T_{MN}=760$ K which is not consistent with a constant τ_{at} value in Eq. (5) independent of the defect activation energy. This is instead the signature of a Meyer–Neldel (MN), or compensation, dependence [37] suggesting that τ_{at} is exponentially linked to E_d as $\tau_{00}\exp(-E_d/kT_{MN})$ [38, 39]. The MN rule has been reported for a large variety of processes [39]. It emerges in defect annealing [39, 40], crystallization [41], phase segregation [42] and transport in amorphous semiconductors [39, 40, 43-45]. The rule basically describes a compensation effect where processes with large activation energy benefit from a relatively small pre-exponential time τ_0 . This dependence may be explained taking into account that when the barrier energy E_d is large compared to the available energy quanta (e.g., phonons), the activation energy E_d should be provided by piling-up multiple elemental excitations. The number of different combinations which may be followed to assembly $n=E_b/h\omega_0$ quanta among those N available in the sample volume, makes the free-energy barrier including an

entropic term which scales almost as $n \log N$, thus leading to the MN rule [39]. The energy of the elemental excitation can be estimated as $kT_{MN}=65$ meV, thus pointing to the role of optical phonons [38, 39]

Figure 10 shows the pre-exponential times τ_0 extracted from Fig. 9 as a function of E_A . Data agree with the MN exponential law and with data extracted for glass transition/crystallization in several metallic glasses [39] and for defect annealing in a-Si:H. [40] Interestingly, Fig. 9 shows that crystallization times t_x from [46] are in good agreement with τ_{SR} for $R^*=100$ M Ω and in Fig. 10 the estimated pre-exponential time t_{0x} falls almost on the same straight line of SR data. These results suggest that crystallization occurs by the same many-body thermal-excitation process as SR, the only difference being the energy barrier, while the different pre-exponential time constant can be well accounted for by the same MN rule.

4. CONCLUSIONS

Investigations of carrier transport and threshold switching in PCM cells have opened the way to the development of a comprehensive and unified physical picture which is able to quantitatively account for a large variety of experimental results and physical effects like the PF conduction of the amorphous in the pre-switching regime, the dependence of the conduction activation energy on bias, threshold switching and the threshold voltage dependence on amorphous thickness, the recovery time, the slow drift of both amorphous resistivity and threshold voltage, the gradual increase of the conduction activation energy following defect annihilation. Last but not least SR and crystallization are reconciled within the same basic physical framework being both driven by atomic rearrangements. Novel evidence is provided that the entropic term due to many-body thermal excitation is indeed responsible for the anomalous large values of the crystallization time pre-factor observed in chalcogenide glasses.

5. ACKNOWLEDGMENTS

The work has been supported in part by the Italian Minister for University and Research (FIRBRBIP06YSJJ) and by grants from Numonyx and Intel Corporation. The authors would like to thank S. Lavizzari, D. Fugazza and M. Boniardi of Politecnico di Milano; A. Redaelli, F. Pellizzer, A. Pirovano, and R. Bez of Numonyx; D. Kau and G. Spadini of Intel Corporation for useful discussions and suggestions.

REFERENCES

1. S. Lai: "Non-Volatile Memory Technologies: The Quest for Ever Lower Cost", IEEE International Electron Device Symposium IEDM, Digest of Technical Papers (2008) 11
2. D.-H. Kang et al.: "Two-bit Cell Operation in Diode-Switch Phase Change Memory Cells with 90nm Technology", 2008 Symposium on VLSI Technology, Digest of Technical Papers (2008) 98
3. S. Eilert, M. Leinwander, G. Crisenza: "Phase Change Memory: A new memory enables new memory usage models", IEEE International Memory Workshop, Digest of Technical Paper (2009) 72
4. C. D. Wright, M. Armand, M. M. Aziz, R. A. Cobley, S. Sendaker, and W. Yu: "Simulation studies on electrical, thermal, and phase-change behavior of GeSbTe based memory devices", Proceedings of EPCOS 2003. [Online]. Available: http://www.epcos.org/library/papers/pdf_2003/Wright.pdf
5. A. L. Lacaita: "Progress of Phase Change Non Volatile Memory Devices", Proceedings of EPCOS 2006. [Online]. Available: http://www.epcos.org/library/papers/pdf_2006/pdf_Invited/Lacaita.pdf
6. S. R. Ovshinsky: "Reversible Electrical Switching Phenomena in Disordered Structures", Phys. Rev. Lett. **21** (1968) 1450
7. D. Adler, H. Henisch, and N. Mott: "The mechanism of threshold switching in amorphous alloys", Rev. Mod. Phys. **50** (1978) 209
8. D. Adler, M. S. Shur, M. Silver, and S. R. Ovshinsky: "Threshold switching in chalcogenide glass thin-films", J. Appl. Phys. **51** (1980) 3289
9. A. Pirovano, A. L. Lacaita, A. Benvenuti, F. Pellizzer, and R. Bez: "Electronic Switching in Phase Change Memories", IEEE Trans. Electron Devices **51** (2004) 452
10. V. G. Karpov, Y. A. Kryukov, S. D. Savransky, and I. V. Karpov: "Nucleation switching in phase change memory", Appl. Phys. Lett. **90** (2007) 123504
11. D. Ielmini and Y. Zhang: "Analytical model for subthreshold conduction and threshold switching in chalcogenide-based memory devices", J. Appl. Phys. **102** (2007) 054517
12. A. Redaelli, A. Pirovano, A. Benvenuti and A. L. Lacaita: "Threshold switching and phase transition numerical models for phase change memory simulations", J. Appl. Phys. **103** (2008) 111101

13. S. Lavizzari, D. Ielmini, D. Sharma and A. L. Lacaita: Transient effects of delay, switching and recovery in phase change memory (PCM) devices”, IEEE International Electron Device Meeting IEDM, Technical Digest (2008) 215
14. N. F. Mott and E. A. Davis: “Electronic Processes in Non-Crystalline Materials”, Clarendon, Oxford, 1979.
15. R. A. Street and N. F. Mott: “States in the Gap in Glassy Semiconductors”, Phys. Rev. Lett. **35** (1975) 1293
16. S. R. Ovshinsky: “Localized States in the Gap of Amorphous Semiconductors”, Phys. Rev. Lett. **36** (1976) 1469
17. A.K.Jonsher and A.A. Ansari: “Photo-currents in silicon monoxide films”, Phil. Mag. **23** (1971) 205.
18. A.K.Jonsher: Energy losses in hopping conduction at high electric fields”, J. Phys. C: Solid St. Phys. **4** (1971) 1331
19. A. Pirovano, A. L. Lacaita, F. Pellizzer, S.A. Kostylev, A. Benvenuti and R. Bez: “Low field amorphous state resistance and threshold voltage drift in chalcogenide materials”, IEEE Trans. Electron Devices **51** (2004) 714
20. D. Ielmini and Y. Zhang: “Evidence of trap-limited transport in the subthreshold conduction regime of chalcogenide glasses”, Appl. Phys. Lett. **90**, (2007) 192102.
21. D. Ielmini: “Threshold switching mechanism by high-field energy gain in the hopping transport of chalcogenide glasses”, Phys. Rev. B, Condens. Matter **78** (2008) 035308
22. U. Russo, D. Ielmini, A. Redaelli, and A. L. Lacaita: Intrinsic Data Retention in Nanoscaled Phase-Change Memories—Part I: Monte Carlo Model for Crystallization and Percolation”, IEEE Trans. Electron Devices **53** (2006) 3032
23. A. Redaelli, A. Pirovano, I. Tortorelli, D. Ielmini, Member, IEEE, and A. L. Lacaita: “A Reliable Technique for Experimental Evaluation of Crystallization Activation Energy in PCMs”, IEEE Trans. Electron Devices **29** (2008) 41
24. D. Ielmini, A. L. Lacaita and D. Mantegazza: “Recovery and Drift Dynamics of Resistance and Threshold Voltages in Phase-Change Memories”, IEEE Trans. Electron Devices **54**, (2007) 308
25. G. P. Tiwari, R. V. Ramanujan, M. R. Gonalb, R. Prasad, P. Raj, B. P. Badguzar, and G. L. Goswami: “Structural relaxation in metallic glasses”, Mater. Sci. Eng. A, **304-306** (2001) 499
26. S. Roorda, W. C. Sinke, J. M. Poate, D. C. Jacobson, S. Dierker, B. S. Dennis, D. J. Eaglesham, F. Spaepen, and P. Fuoss: “Structural relaxation and defect annihilation in pure amorphous silicon,” Phys. Rev. B, Condens. Matter, **44** (1991) 3702
27. E. P. Donovan, F. Spaepen, D. Turnbull, J. M. Poate, and D. C. Jacobson: “Calorimetric studies of crystallization and relaxation of amorphous Si and Ge prepared by ion implantation” J. Appl. Phys. **57** (1985) 1795
28. M. Hishimaru, I.-T. Bae, Y. Hirotsu, S. Matsumura, and K. E. Sickafus: “Structural relaxation of amorphous silicon carbide”, Phys. Rev. Lett. **89** (2002) 055502
29. S. O. Kasap and S. Yannacopoulos: “Kinetics of structural relaxations in glassy semiconductor a-Se”, J. Mater. Res. **4** (1989) 893
30. K. Koughia, Z. Shakoor, S. O. Kasap, and J. M. Marshall: “Density of localized electronic states in a-Se from electron time-of-flight photocurrent measurements”, J. Appl. Phys. **97** (2005) 033706
31. J. M. Saiter, “Physical ageing in chalcogenide glasses,” J. Optoelectron. Adv. Mater. **3** (2001) 685
32. J. A. Kalb, M. Wuttig, and F. Spaepen: “Calorimetric measurements of structural relaxation and glass transition temperatures in sputtered films of amorphous Te alloys used for phase change recording”, J. Mater. Res. **22** (2007) 748
33. V. A. Khonik, K. Kitagawa, and H. Morii: “On the determination of the crystallization activation energy of metallic glasses”, J. Appl. Phys. **87** (2000) 8440
34. D. Ielmini, D. Sharma, S. Lavizzari, and A. L. Lacaita: “Physical mechanism and temperature acceleration of relaxation effects in phase-change memory cells”, IEEE International Reliability Physics Symposium IRPS, Digest of technical Papers (2008) 597.
35. D. Ielmini, S. Lavizzari, D. Sharma and A. L. Lacaita: “Physical interpretation, modeling and impact on phase change memory (PCM) reliability of resistance drift due to chalcogenide structural relaxation”, IEEE International Electron Device Meeting – IEDM, Technical Digest (2007) 939
36. S.Lavizzari, D. Ielmini, D. Sharma, and A. L. Lacaita: “Reliability Impact of Chalcogenide-Structure Relaxation in Phase-Change Memory (PCM) Cells—Part II: Physics-Based Modeling”, IEEE Trans. Electron Devices **56** (2009) 1078
37. W. Meyer and H. Neldel, Z. Tech. Phys. (Leipzig) **12**, (1937) 588.
38. A. Yelon and B. Movaghar: “Microscopic explanation of the compensation (Meyer Neldel) rule “, Phys. Rev. Lett. **65**, (1990) 618
39. A. Yelon, B. Movaghar, and H. M. Branz: “Origin and consequences of the compensation (Meyer Neldel) law “, Phys. Rev. B **46**, (1992) 12244
40. R. Crandall, “Defect relaxation in amorphous silicon: Stretched exponentials, the Meyer-Neldel rule, and the Staebler-Wronski effect,” Phys. Rev. B **43** (1991) 4057
41. N. Mehta, A. Kumar: “Pre-exponential factor of Arrhenius equation for the isothermal crystallization of some Se-Ge, Se-In and Se-Te chalcogenide glasses“, J. Mater. Sci. **42** (2007) 490
42. A. Kumar Singh, N. Mehta, K. Singh: “Correlation between Meyer-Neldel rule and phase separation in $\text{Se}_{98-x}\text{Zn}_2\text{In}_x$ chalcogenide glasses “, Curr. Appl. Phys. **9** (2009) 807
43. W.B. Jackson: “Connection between the Meyer-Neldel relation and multiple-trapping transport“, Phys. Rev. B **38** (1988) 3595
44. R. Widenhorn, A. Rest, E. Bodegom: “The Meyer-Neldel rule for a property determined by two transport mechanisms“, J. Appl. Phys. **91** (2002) 6524
45. S. Savranski, I.V. Karpov: “Investigation of SET and RESET states resistance in ohmic regime for phase-change memory“, in Proceedings of Mater. Res. Soc. Symp. (2008) 1072
46. A. Redaelli, D. Ielmini, U. Russo, and A. L. Lacaita: “Intrinsic data retention in nanoscaled phase-change memories - Part II: Statistical analysis and prediction of failure time“, IEEE Trans. Electron Devices **53** (2006) 3040
47. D. Ielmini, M. Boniardi, A.L. Lacaita, A. Redaelli, A. Pirovano: “Unified mechanisms for structural relaxation and crystallization in phase-change memory devices”, Microelectron. Engineering **86** (2009) 1942

Biographies

Andrea L. Lacaita. Born in 1962. He received the Laurea degree (*cum laude*) in Nuclear engineering from the Politecnico di Milano, Milano, Italy in 1985. Since 1992, he has been an EE Professor at the Politecnico di Milano, Milano, full professor of electronics since 2000. From 2006 to 2008, he has served as the Department Chair of the Dipartimento di Elettronica ad Informazione and member of the Academic Senate from 2007 to 2008.. Previously, he was a Researcher with the CNR (Italian National Research Council) from 1987 to 1992. He was a Visiting Scientist/Professor with the AT&T Bell Laboratories, Murray Hill, NJ, from 1989 to 1990, and the IBM T. J. Watson Research Center, Yorktown Heights, NY, in 1999.

In 1992, he established the Micro and Nanoelectronics Laboratory, starting with two research lines: one addressing carrier transport and quantum effects in submicrometer MOSFETs and the other aiming at analog integrated circuit design. In the field of device physics, he has contributed to study quantum effects as well as experimental characterization techniques and numerical models of nonvolatile memories, both Flash and emerging (PCM, RRAM). He is the coauthor of more than 200 papers published in international journals or presented to international conferences, patents, and several educational books in electronics. He has served in several scientific committees such as IEEE-IEDM (2001–2002), IEDM European Chair (2003–2004), ESSDERC (2005, 2009), and IEEE VLSI Symposium (2005–2008). He is IEEE Fellow.

Daniele Ielmini was born in 1970. He received the Laurea (*cum laude*) and Ph.D. degrees in nuclear engineering from Politecnico di Milano, Milano, Italy, in 1995 and 1999, respectively. Since 1999, he has been with the Dipartimento di Elettronica e Informazione, Politecnico di Milano, where he became an Assistant Professor in 2002. He is also with the Italian Universities Nanoelectronics Team, Politecnico di Milano. In 2006, he was a Visiting Scientist at Intel Corporation, Santa Clara, CA, and the Center for Integrated Systems, Stanford University, Stanford, CA. He has been working in the field of CMOS dielectric reliability and in the modeling and characterization of Flash and emerging nonvolatile memories, including nanocrystal memories, charge-trap memories, phase-change memories (PCMs) and resistive-switching memories (RRAMs). He is author/coauthor of one book chapter and more than 120 publications in international journals and international conference proceedings. He has been serving in the Technical Committees of IRPS (2006-2008), SISC (2008) and IEDM (2008-2009).